Bull. Mater. Sci., Vol. 31, No. 3, June 2008, pp. 573–577. © Indian Academy of Sciences.

In situ high temperature XRD studies of ZnO nanopowder prepared via cost effective ultrasonic mist chemical vapour deposition

PREETAM SINGH, ASHVANI KUMAR, AJAY KAUSHAL, DAVINDER KAUR*, ASHISH PANDEY† and R N GOYAL†

Department of Physics and Centre of Nanotechnology, †Department of Chemistry and Centre of Nanotechnology, Indian Institute of Technology Roorkee, Roorkee 247 667, India

Abstract. Ultrasonic mist chemical vapour deposition (UM–CVD) system has been developed to prepare ZnO nanopowder. This is a promising method for large area deposition at low temperature inspite of being simple, inexpensive and safe. The particle size, lattice parameters and crystal structure of ZnO nanopowder are characterized by *in situ* high temperature X-ray diffraction (XRD). Surface morphology of powder was studied using transmission electron microscopy (TEM) and field emission electron microscope (FESEM). The optical properties are observed using UV-visible spectrophotometer. The influence of high temperature vacuum annealing on XRD pattern is systematically studied. Results of high temperature XRD showed prominent 100, 002 and 101 reflections among which 101 is of highest intensity. With increase in temperature, a systematic shift in peak positions towards lower 2θ values has been observed, which may be due to change in lattice parameters. Temperature dependence of lattice constants under vacuum shows linear increase in their values. Diffraction patterns obtained from TEM are also in agreement with the XRD data. The synthesized powder exhibited the estimated direct bandgap (E_g) of 3·43 eV. The optical bandgap calculated from Tauc's relation and the bandgap calculated from the particle size inferred from XRD were in agreement with each other.

Keywords. High temperature XRD; ZnO nanopowder; ultrasonic mist chemical vapour deposition.

1. Introduction

ZnO has attracted much attention in the last few decades due to its wide variety of applications in optoelectronic devices. ZnO is a semiconductor with a wide bandgap of about 3·4 eV, which is tuned over a large energy range i.e. it is transparent in the visible region with high luminous transmittance. The stable structure of ZnO is wurtzite, in which four atoms of oxygen in tetrahedral coordination surround each atom of zinc. Combined with the high conductivity that can be achieved by doping, this leads to applications in surface acoustic wave devices and transparent conducting electrodes as reported by Raju and Rao (1991). It is a strong piezoelectric, and piezoelectric properties can change the characteristics of potential energy barriers at interfaces. The resulting piezoresistance is exploited in metal oxide varistors which can dissipate large amounts of power in short response times and are commonly found in electrical surge protectors as reported by Wang (2004). Semiconductor nanostructures are promising candidates for future electronic and photonic devices. Lee (2002) suggested that nanostructures based on wide bandgap semiconductors such as GaN and ZnO are of particular interest because of their applications in short wavelength light emitting devices and field emission devices. ZnO is characterized by a large exciton binding energy (~60 meV) and the thermal energy at room temperature (~25 meV) and therefore, allows stable existence of excitons at room temperature as reported by Chia *et al* (2003). Various methods have been used for the deposition of ZnO like sol–gel by Kim *et al* (2004), spray pyrolysis by Studenikin *et al* (1998), metal organic chemical vapour deposition by Ohya *et al* (2001) and so on. Because nanostructure ZnO has many applications in industrial area so the preparation of nanosize ZnO is an important issue. For this purpose ultrasonic mist-chemical vapour deposition (UM–CVD) is a simple and inexpensive method for the deposition of nanoparticles.

In this paper, we report the structural and optical properties of ZnO nanopowder deposited via cost effective UM–CVD technique. Liquid solution of concentration, 0·1 M, was prepared from the dissolution of zinc nitrate hydrate in distilled water and was sprayed using an ultrasonic generator operated to an atomizing frequency of 1·7 MHz. The produced droplets were then carried into the chamber by air carrier gas and pyrolyzed at a predetermined temperature. As a result, zinc oxide powder was formed. *In situ* high temperature X-ray diffraction studies were done for the first time in the temperature range varying from room temperature to 700°C to study the effect of temperature on phase, crystallite size and lattice constants of ZnO nanocrystalline powder.

*Author for correspondence (dkaurfph@iitr.ernet.in)

2. Experimental

ZnO powder was prepared using the modified ultrasonic spray process. The set up was composed of three zones. The first was the ultrasonic spray zone which consists of the mist generating system of liquid source with ultrasonic atomizer and misted droplet carrying system with air carrier gas. The second was the heating zone in which the misted droplet was pyrolyzed in a preheated reactor. The last and the third zone was for the trapping of produced powder. To prepare ZnO nanopowder, zinc nitrate [$Zn(NO_3)_2{\cdot}6H_2O$] (purity > 99%, Sigma Aldrich, USA) was used as precursor. The solution was prepared from dissolution of metal nitrate hydrate in pure water to a concentration of 0·1 M. The aqueous zinc nitrate solution was delivered into the reactor by liquid atomization. The atomized droplets containing the precursor were passed through a reactor and collected on a special geometry.

The orientation and crystallinity of the powder were studied using Bruker AXS C-8 advanced diffractometer with high temperature attachment in θ–2θ geometry. The high temperature stage allows samples to be measured at tightly controlled temperatures from room temperature to 1600°C in open air, under vacuum, or in a purge gas. The surface topography and microstructure were studied using field emission scanning electron microscope (FESEM). The micrographs and diffraction pattern of nanopowder was studied using transmission electron microscope (Philips EM400). Perkin Elmer Lambda 25 UV-Visible spectrometer was used to study the optical properties of nanopowder.

3. Results and discussion

The results of *in situ* high temperature X-ray diffraction in vacuum for ZnO nanopowder at increasing temperature from room temperature to 700°C are shown in figure 1.

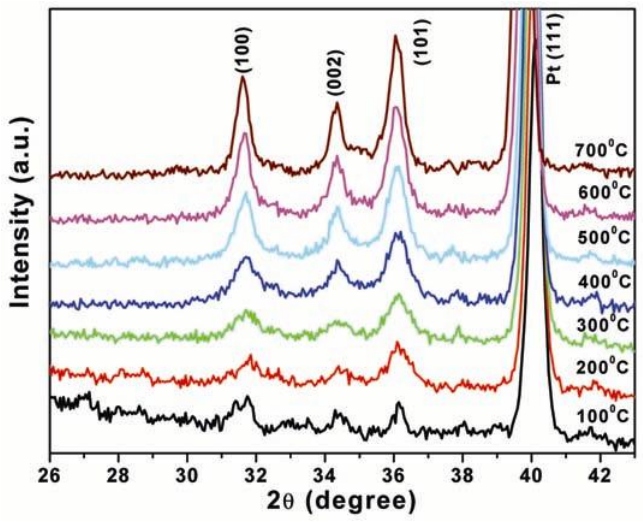

Figure 1. XRD spectra of ZnO nanoparticles at various temperatures.

ZnO nano powder mixed with zapon lacquer is applied on a platinum strip, which is used as a sample holder cum heater for high temperature XRD. It has been observed that the XRD peak broadening decreases with increase of temperature. The observed reflections were (100), (002) and (101) which were similar to the observed reflections in ZnO bulk. The intensity of these reflections increases with rise in temperature. It is well known that the lattice parameters are temperature dependent, i.e. an increase in temperature leads to expansion of the lattice as reported by Lamber *et al* (1995) and Banerjee *et al* (2003). It was observed that the particle size and lattice parameters increased with increasing temperature as shown in table 1.

The increase of the lattice parameter of ZnO nanopowder with increase in temperature was calculated using the equation

$$\frac{1}{d_{101}^2} = \frac{4}{3}\left(\frac{1}{a^2}\right) + \frac{1}{c^2},$$

where d is the interplanar distance, a and c are the lattice parameters (being hexagonal structure, $c/a = \sqrt{8/3}$). The XRD results indicated that the synthesized ZnO powders had the pure wurtzite structure with lattice parameters, a and c, of 3·244 and 5·297 nm, respectively at room temperature. The XRD spectra were used to calculate the crystallite size of ZnO nanoparticles with increase in temperature using Scherrer's formula from Cullity (1970)

$$d = \frac{0{\cdot}9\lambda}{B\cos\theta_B},$$

where λ, θ_B and B are the X-ray wavelength (1·54056 Å), Bragg diffraction angle and line width at half maximum, respectively. We have also incorporated the instrumental broadening for size calculations. The lattice parameters (a and c) and particle size as a function of temperature are shown in figure 2(a, b) and it was observed that there is a continuous increase in the lattice parameter and particle size with temperature as shown in table 1. It was found that the crystallite size of ZnO nanopowder was around 15·2 nm at 100°C which increased to 21·8 nm when the sample was heated to 700°C.

According to Ostwald ripening the increase in the particle size is due to the merging of the smaller particles into larger ones as suggested by Nanda *et al* (2002) and is a result of potential energy difference between small and large particles and can occur through solid state diffusion. To examine this let us consider a particle, P, of diameter, R_0. The particle, P, can be changed into n smaller identical unit cells of edges, a and c without changing its volume

$$\frac{4}{3}\pi\left(\frac{R_0}{2}\right)^3 = nV,$$

where $V = 3\sqrt{3}/2a^2c$ (for hexagonal structure) i.e.

Table 1. Various measured properties of ZnO nanoparticles.

Temperature (°C)	Particle diameter, $R_0 \pm 0{\cdot}5$ (nm)	Lattice parameter, a(Å)	Lattice parameter, c(Å)	No. of unit cells, n
100	15·2	3·244	5·297	12688
200	16·3	3·245	5·299	15631
300	17·8	3·247	5·302	20319
400	19·6	3·249	5·305	27079
500	19·7	3·250	5·307	27468
600	20·2	3·252	5·310	29560
700	21·8	3·253	5·312	37120

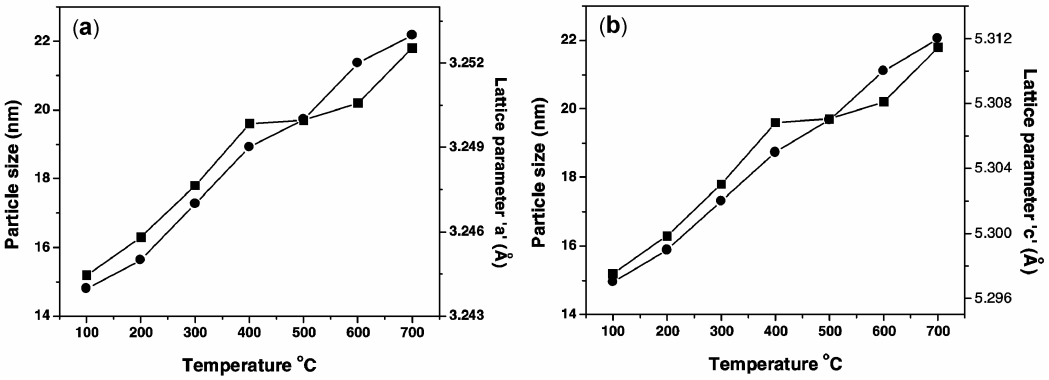

Figure 2. (**a**) Variation of particle size and lattice parameter, a and (**b**) variation of particle size and lattice parameter c as a function of temperature.

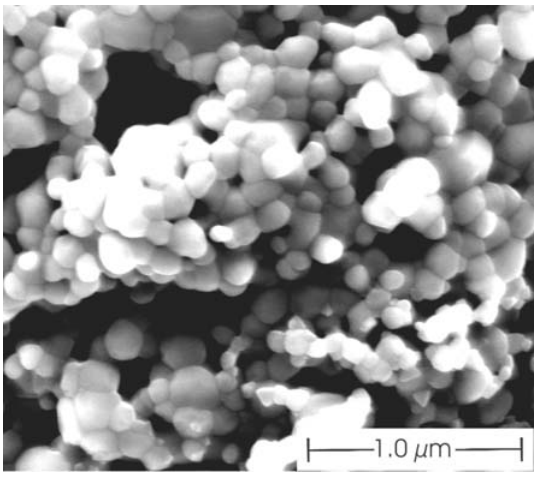

Figure 3. FESEM image of ZnO nanopowder.

$$n = \frac{4}{3}\pi\left(\frac{R_0}{2V}\right)^3.$$

It is evident from table 1 that the number of unit cells in the particle increases with an increase in temperature even after incorporating the increase in lattice parameter. This can be attributed to the Ostwald ripening according to which large particles grow at the expense of smaller ones. The morphology of ZnO nanopowder as revealed by FESEM (figure 3) showed nanoparticles of size, ~50–100 nm.

The morphology and structure of powder was further investigated by TEM. Bright field TEM images and the corresponding diffraction pattern for ZnO nanopowder were shown in figure 4. The sample was scanned in all zones before the picture was taken. The micrographs revealed that the particles were nearly spherical in shape. The diffraction pattern shows spotty ring pattern without any additional diffraction spots and rings of secondary phases revealing their highly crystalline ZnO wurtzite structure. Three fringe patterns were observed with plane distances of 2·79, 2·58 and 2·44 Å in the electron diffraction pattern which corresponds to 100, 002 and 101 planes of pure wurtzite hexagonal structure of ZnO.

The optical transmission spectra of the ZnO nanoparticle was recorded as a function of wavelength in the wavelength range 300–900 nm as shown in figure 5. Transmittance spectra revealed that the average value of transmittance was about 55% in the visible range of electromagnetic radiation. The transmittance is expected to depend on several factors, such as oxygen deficiency, surface roughness, and impurity centres. The lower value of transmittance in case of ZnO nanopowder could be due to light scattering at the rough surface. Transmittance spectra also presented a sharp ultraviolet cut-off at ~310 nm which reflects that in case of ZnO powder the

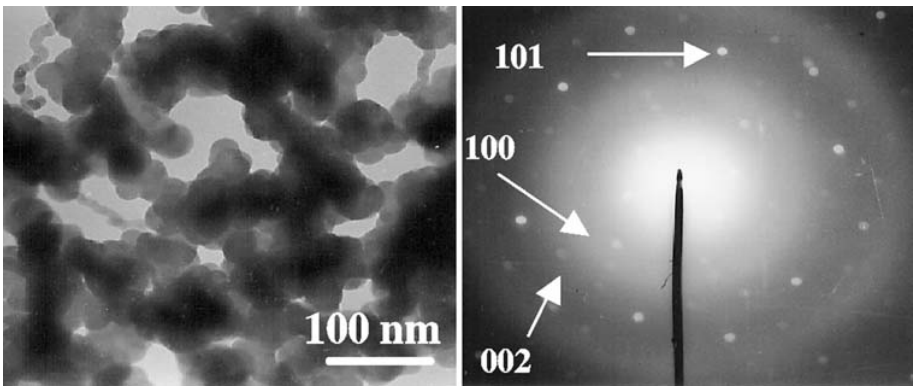

Figure 4. TEM images and corresponding diffraction pattern of ZnO nanoparticles.

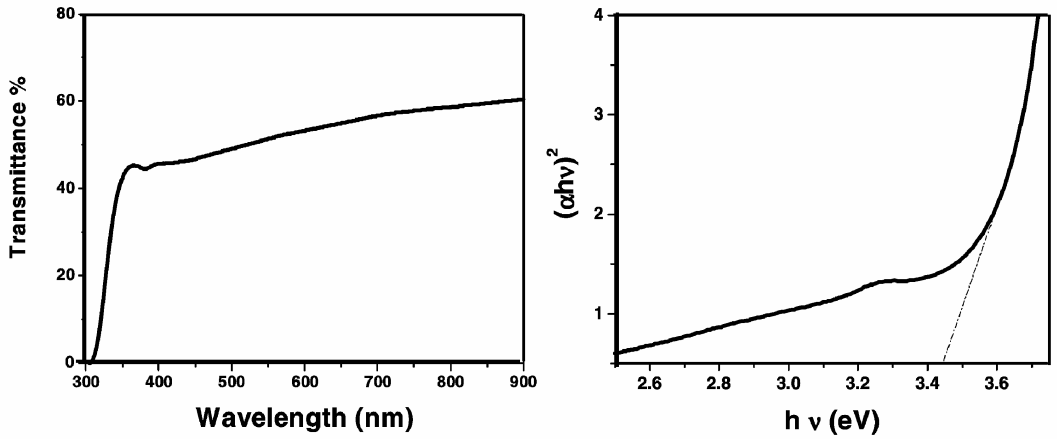

Figure 5. (**a**) Optical transmittance spectra and (**b**) energy bandgap of ZnO nanoparticles.

absorption edge of transmittance shifts to longer wavelength region and there is an increase in the optical absorption in the UV region.

In order to calculate the direct bandgap, we used the Tauc's (1994) relationship as follows

$$\alpha h\nu = A(h\nu - E_g)^n,$$

where α is the absorption coefficient, A, a constant, h is Planck's constant, ν the photon frequency, E_g the optical bandgap and n is 1/2 for direct semiconductor. An extrapolation of the linear region of a plot of $(\alpha h\nu)^2$ on the y-axis versus photon energy ($h\nu$) on the x-axis gives the value of the optical bandgap, E_g. Since $E_g = h\nu$, when $(\alpha h\nu)^2 = 0$. The calculated bandgap was found to be near 3·43 eV of the ZnO nanopowder, which is greater than the reported bandgap value of ZnO bulk i.e. $E_g = 3{\cdot}37$eV (Zu *et al* 1997). The difference in the bandgap values ranging from 3·1–3·3 eV is one of the curious features of the literature on ZnO. Srikant and Clarke (1998) investigated the optical bandgap of ZnO single crystals at room temperature using a variety of optical techniques (i.e. conventional reflection and transmission absorption measurement, spectroscopic ellipsometry, Fourier transform infared spectroscopy and photoluminescence) and reported three different E_g which is greater than the bandgap in the case of bulk values of 3·1, 3·2 and 3·3 eV. They concluded that the room temperature bandgap of ZnO was 3·3 eV, whereas reports of an apparent bandgap at 3·1 and 3·2 eV were due to the existence of a valence band–donor transition at 3·15 eV which can dominate the absorption spectrum when the bulk, as distinct from the surface, of a single crystal is probed.

For the sake of comparison we estimated the bandgap of these films deposited on glass from the relation given by Brus (1984)

$$E_g = E_g^0 + \frac{h^2}{8\mu R^2},$$

where E_g^0 was the energy bandgap for bulk material, R was the radius of the particles calculated from XRD data and $1/\mu = 1/m_e + 1/m_h$ (m_e and m_h being the electron and hole effective masses, respectively). Here the reduced mass of the exciton was $0{\cdot}242m_0$ as reported by Singh *et al* (2007). Thus we obtain $E_g = E_g^0 + 1{\cdot}545R^{-2}$ (nm). The

values calculated from the above given formula was found to be 3·236 eV which is in agreement with the optical bandgap value calculated from the Tauc relation.

4. Conclusions

In summary, we have used ultrasonic mist chemical vapour deposition technique to prepare ZnO nanopowder. The technique is simple and inexpensive method allowing the large area deposition at low temperature. From the XRD and TEM analysis, it was confirmed that the resultant particles of nanopowder were pure ZnO with hexagonal (wurtzite) structure. High temperature XRD also confirmed that the ZnO nanoparticles were stable not only at room temperature but at high temperature as well. We had also studied the variation in lattice parameters with temperature. A linear increase in lattice parameters with temperature along with increase in the size of the grains was observed. Optical studies showed that the transmittance and the bandgap of the films deposited on glass increased with increasing the deposition temperature and the bandgap calculated from Tauc relation were in agreement with the bandgap calculated from XRD.

Acknowledgement

We are thankful to the Department of Science and Technology, New Delhi, for financial support under the scheme 'Nanoscience and Technology Initiatives (NSTI)' with reference No. DST 238.

References

Banerjee R, Sperling E A, Thompson G B, Fraser H L, Bose S and Ayyub P 2003 *Appl. Phys. Lett.* **82** 4250
Brus L E 1984a *J. Chem. Phys.* **80** 1
Brus L E 1984b *J. Chem. Phys.* **80** 4403
Chia C H, Makino T, Tamura K, Segawa Y, Kawasaki M, Ohtomo A and Koinuma H 2003 *Appl. Phys. Lett.* **82** 1848
Cullity B D 1970 *Elements of X-ray diffraction* (Addison-Wesley) p. 102
Kim Y M, Yoon M, Park I W, Park Y J and Lyou J H 2004 *Solid State Commun.* **129** 175
Lamber R, Wetjen S and Jaeger N I 1995 *Phys. Rev.* **B51** 10968
Lee C J, Lee T J, Lyu S C, Zhang Y, Ruh H and Lee H 2002 *Appl. Phys. Lett.* **81** 3648
Makino T, Segawa Y, Kawasaki M, Ohtomo A, Shoroki R, Tamura K, Yasuda T and Koinuma H 2001 *Appl. Phys. Lett.* **78** 1237
Nanda K K, Kruis F E and Fissan H 2002 *Phys. Rev. Lett.* **89** 256103
Ohya Y, Niwa T, Ban T and Takahashi Y 2001 *Jpn J. Appl. Phys.* **40** 29
Raju A R and Rao C N R 1991 *Sensor Actuator* **B3** 305
Singh P, Chawla A K, Kaur D and Chandra R 2007 *Mater. Lett.* **61** 2050
Srikant V and Clarke D R 1998 *J. Appl. Phys.* **83** 5447
Studenikin S A, Golego N and Cocivera M 1998 *J. Appl. Phys.* **84** 2287
Tauc J (ed.) 1974 *Amorphous and liquid semiconductor* (New York: Plenum Press)
Wang J L 2004 *J. Phys. Condens. Matter* **16** R829
Wood V E and Austin A E 1975 *Magnetoelectric interaction phenomena in crystals* (London: Gordon and Breach)
Zu P, Tang Z K, Wong G K L, Kawasaki M, Ohtomo A, Koinuma H and Segawa Y 1997 *Solid State Commun.* **103** 459